DYNAMO ACTION IN PRECESSING CYLINDERS

NORE C.[1], LEORAT J.[2], GUERMOND J.-L.[3], CAPPANERA L.[1], LUDDENS F.[1,4]
Affiliation: [1]*LIMSI-CNRS/*Bâtiment 508, BP 133, 91403 Orsay cedex, France et Université Paris-Sud, 91405 Orsay cedex, France, [2]*Luth*, Observatoire de Paris-Meudon, place Janssen, F-92195-Meudon, France, [3]Department of Mathematics, Texas A&M University, 3368 TAMU, College Station, Texas 77843-3368, USA,
[4]*IMB* Université Bordeaux I, 351 cours de la Libération, 33405 Talence cedex, France.
e-mail address of corresponding author: caroline.nore@ limsi.fr

Abstract : It is numerically demonstrated by means of a magnetohydrodynamic (MHD) code that precession can trigger the dynamo action in a cylindrical container. When the angle between the spin axis and the precession axis is fixed to pi/2, two spinning ways can be explored: either the symmetry axis of the cylinder is parallel to the spin axis (denoted as the *axial spin* case) or it is perpendicular to the spin axis (denoted as the *equatorial spin* case). In both cases, when the Reynolds number, based on the radius of the cylinder and its spin angular velocity, increases, the flow, which is initially centro-symmetric, loses its stability and bifurcates to a quasi-periodic motion. This unsteady and asymmetric flow is shown to be capable of sustaining dynamo action in the linear and nonlinear regimes. The magnetic field thus generated is mainly quadrupolar in the *axial spin* case while it is mainly dipolar in the *equatorial spin* case. These numerical evidences of dynamo action in a precessing cylindrical container may be useful for the design of new dynamo experiments, such as the one planned at the DRESDYN facility in Germany [1].

1. Introduction

The possible contribution of precession to dynamo action is a long-standing debate (see for example [2]). Modern astrophysical observations of some planetary dynamos can contribute to resolving this issue, although definite evidence is still lacking. Because of the large computing resources required, it was only recently that numerical computations could demonstrate that dynamo action occurs in different precessing containers: spherical [3] and spheroidal [4] ones. Since neither shape is convenient for large-scale experiments, it is instructive to investigate whether similar results can be obtained in cylindrical containers. We use a nonlinear magnetohydrodynamic (MHD) code denoted SFEMaNS (for Spectral / Finite Elements for Maxwell and Navier-Stokes equations, [5]), which is able to integrate nonlinear MHD equations for incompressible fluids in heterogenous domains (with spatial distributions of electrical conductivity or magnetic permeability) with axisymmetric interfaces embedded in a vacuum. SFEMaNS is based on a spectral method in the azimuthal direction and involves finite elements in meridional planes (see [6] for more details). Six parameters govern the flow: the aspect ratio of the container, the precession angle (angle between the spin axis OS and the precession axis OP), the spin angle (angle between the symmetry axis Oz and the spin axis OS), the precession rate ε (ratio of the precession and spin angular velocity), the Reynolds number Re and the magnetic Reynolds number Rm (see fig. 1). Choosing the container length equal to its diameter, a precession axis orthogonal to the spin axis (precession angle of pi/2) and a precession rate ε=0.15, we are left with two limit configurations: one called *axial spin* for which the spin angle is 0 and the symmetry axis of the cylinder remains fixed in the precession frame (see fig. 1 right) and another one called *equatorial spin* for which the spin angle is pi/2 and the symmetry axis rotates in the precession frame (see fig. 1

left). The purpose of this paper is to examine these two configurations in the hydrodynamical regime varying Re and in the MHD regime varying Re and Rm.
The MHD equations are written:

$$\partial_t \mathbf{u} + (\mathbf{u}\cdot\nabla)\mathbf{u} + 2\varepsilon \mathbf{e}_p \times \mathbf{u} + \nabla p = \frac{1}{R_e}\Delta\mathbf{u} + \mathbf{f},$$
$$\nabla\cdot\mathbf{u} = 0,$$
$$\partial_t \mathbf{h} - \nabla\times(\mathbf{u}\times\mathbf{h}) = \frac{1}{R_m}\Delta\mathbf{h},$$
$$\nabla\cdot\mathbf{h} = 0,$$

where **u**, p and **h** are the velocity field, the pressure and the magnetic field, respectively. **f** is the Lorentz force.

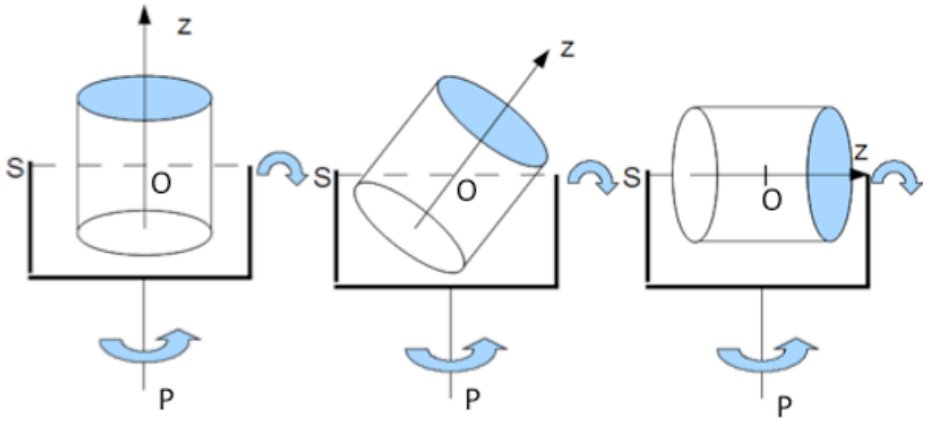

Figure 1: Different ways of spinning for precession driving: (left) equatorial spin (the spin angle is pi/2); (middle) oblique spin; (right) axial spin (the spin angle is 0). OS is the spin axis, OP the precession axis and Oz the symmetry axis.

2. Hydrodynamical study

We have focused on these two limit cases because, in the *axial spin* case, the wall speed is tangent to the wall and only the viscous stress on the wall drives the flow while, in the *equatorial spin* case, the flow can be driven by the pressure on the wall and is therefore inertially driven.
At low Reynolds number, the flow is steady and centro-symmetric, meaning that **u**(**r**)=-**u**(-**r**). At larger Reynolds numbers, the loss of centro-symmetry can be monitored by inspecting the symmetric and antisymmetric components of **u**(**r**,t): $\mathbf{u_s}(\mathbf{r},t)$= 0.5*(**u**(**r**,t)-**u**(-**r**,t)) and $\mathbf{u_a}(\mathbf{r},t)$= 0.5*(**u**(**r**,t)+**u**(-**r**,t)). In the Navier-Stokes simulations reported here, we monitor the time evolution of the total kinetic energy K(t)= 0.5 $\int \mathbf{u}^2$ dV, and of the asymmetric kinetic energy Ka(t)= 0.5 $\int \mathbf{u_a}^2$ dV. Figure 2 compares the energies in the two cases: for the *axial spin* case, the efficiency of the viscous forcing decreases when Re increases; for the *equatorial spin* case, saturation is not achieved yet at Re=2000. The asymmetry ratio is larger in the *equatorial spin* case than in the *axial spin* case. Based on the phenomenological argument that dynamo action is favored by symmetry breaking, it was anticipated that the *equatorial spin* case could generate dynamo action at a lower threshold than the *axial spin* case. However, it is shown below that this intuitive argument is incorrect.

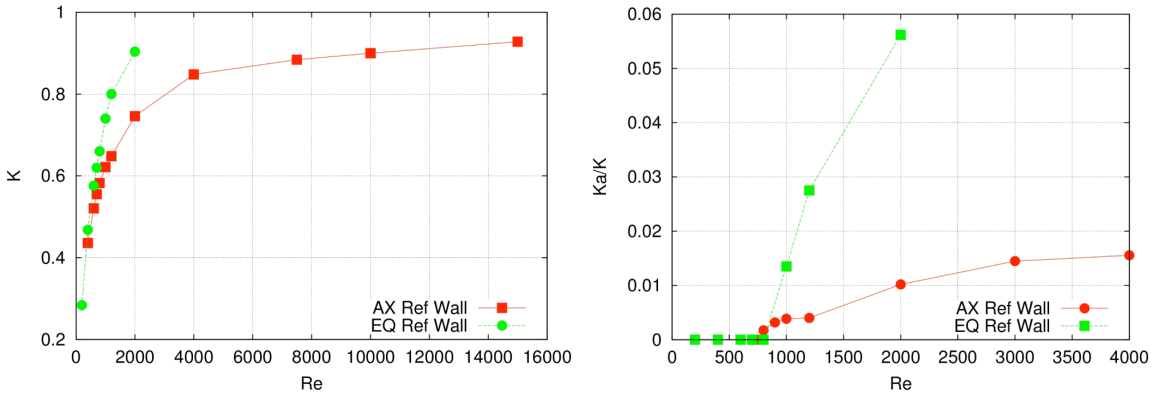

Figure 2: Comparisons between the axial and equatorial spin cases in the reference frame of the wall (also called the *mantle frame*) for a fixed precession rate 0.15: (left) total kinetic energy as a function of Re; (right) asymmetry ratio Ka(t)/K(t) as a function of Re.

3. Dynamo action

The nonlinear MHD problem starts after a small magnetic seed field is added. When the magnetic dissipation is small enough, i.e. for magnetic Reynolds numbers Rm above a critical value $Rm_c(Re)$, dynamo action appears after symmetry breaking of the flow, as was also observed in the spherical and spheroidal dynamos.
In the *axial spin* case, we have found [7] that $Rm_c \approx 750$ at Re=1200. The generated magnetic field is unsteady and mainly quadrupolar. We have varied the Reynolds number and determined the critical curve $Rm_c(Re)$ shown in fig. 3. The critical magnetic Reynolds number presents a non-monotonic variation with Re and admits a minimum value for Re=1200. It seems that increasing Re leads to an efficiency reduction of the dynamo.

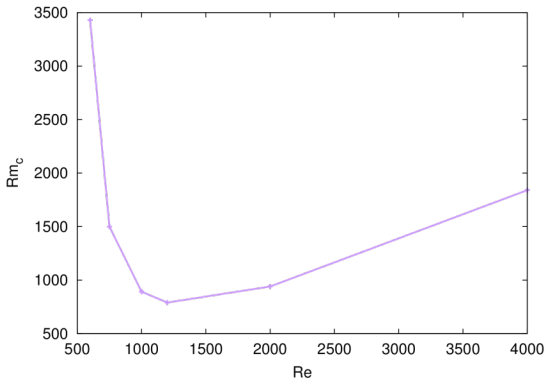

Figure 3: Critical curve $Rm_c(Re)$ in the *axial spin* case.

In the *equatorial spin* case, various MHD runs are performed at Re=1200 for different values of the magnetic Reynolds numbers Rm. The onset of dynamo action is monitored by recording the time evolution of the magnetic energy in the conducting fluid $M(t)= 0.5 \int \mathbf{h}^2 \, dV$. Linear dynamo action occurs when M(t) is an increasing function of time for large times and when the retroaction of the Lorentz force is not active (we impose $\mathbf{f}=0$ in Navier-Stokes equation). The time evolution of M for Rm=1200, 2000 and 2400 is shown on fig. 4 (left). The runs at Rm=2000 and 2400 are done using the velocity and the magnetic fields obtained from the run at Rm=1200 at t=282 as initial velocity and magnetic fields. Linear interpolation of the growthrates gives the critical magnetic Reynolds number $Rm_c \approx 2130$ at Re=1200, i.e. almost three times greater than for the *axial spin* case.

To observe the nonlinear saturation, we have used as initial data the velocity and magnetic fields from the linear MHD run at t=346 at Rm=2400: the velocity field has been kept unchanged but we have multiplied by 400 the amplitude of the magnetic field. Figure 4 (right) shows that M decreases rapidly (in one turnover time, i.e. until t=352) and begins to oscillate thereafter. After restarting the MHD run at t=382 with Rm=2000 and running it until t=428, we observe that M decreases. After restarting the MHD run at t=412 with Rm=1200 and running it until t=446, we observe that the dynamo dies in a short time lapse. A snapshot of the vorticity and the magnetic field lines at Re=1200 and Rm=2400 is shown on fig. 5. We observe a central S-shaped vortex deformed by the precession and connected to the walls through viscous boundary layers. The magnetic energy is dominated by the azimuthal modes m=1,2,3 and the magnetic field lines exhibit a dominant dipolar shape.

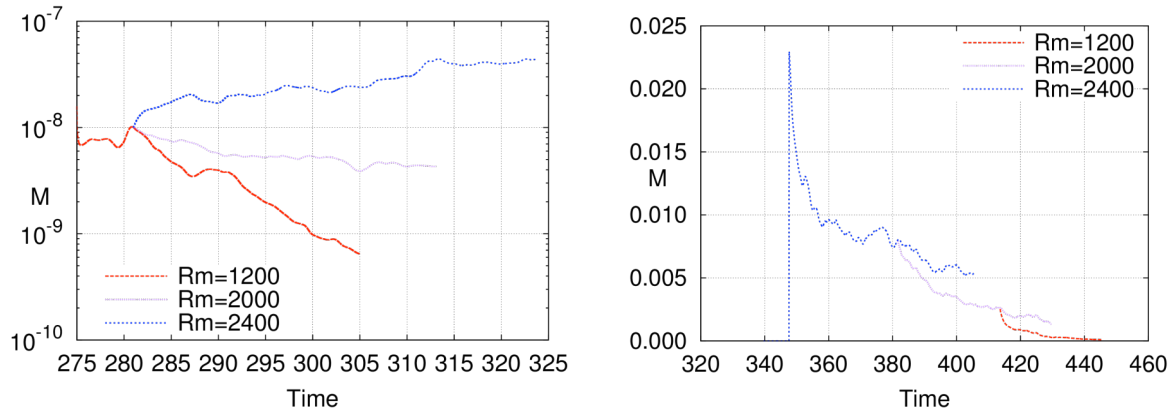

Figure 4: Time evolution of the magnetic energy M in the conducting fluid (left) in the linear regime from t=275 at Re=1200 and various Rm as indicated (in lin-log scale) and (right) in the nonlinear regime for Re=1200 and various Rm as indicated. *Equatorial spin* case.

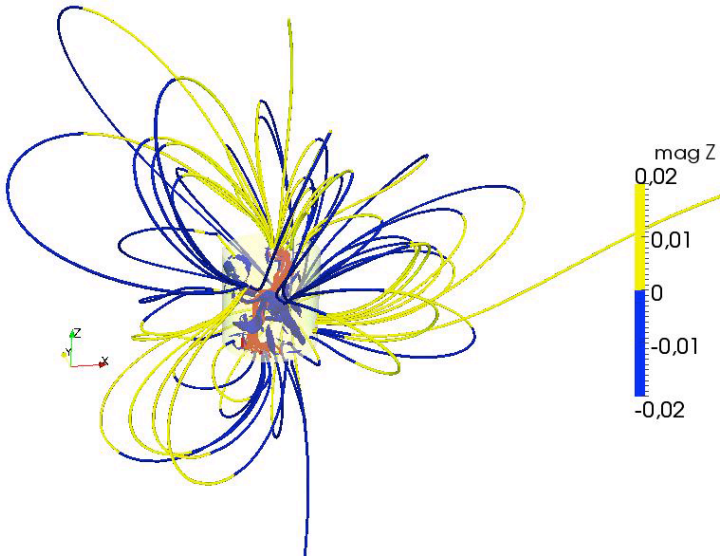

Figure 5: Snapshot at Re=1200 and Rm=2400 of the vorticity field lines (grey/red) and the magnetic field lines colored by the axial component (light grey/yellow for positive vertical magnetic field component and black/blue for negative vertical magnetic field component). The view is seen from the side (Ox is the spin axis, Oz the precession axis). *Equatorial spin* case.

4. Conclusion

We have studied the dynamo capabilities of a precessing cylinder in two limit configurations.

The dynamo threshold found in the *equatorial spin* configuration is greater than that found in the *axial spin* configuration at the same Reynolds number Re=1200. This result is in contrast to the intuition that wall-normal stress would enhance symmetry breaking and would favor dynamo action. The challenge is now to increase the Reynolds numbers in the MHD simulations to more realistic values.

5. References

[1] Stefani, F., Eckert, S., Gerbeth, G., Giesecke, A., Gundrum, Th., Steglich, C., Weier, T., Wustmann, B.DRESDYN - A new facility for MHD experiments with liquid sodiumMagnetohydrodynamics 48, 103-113 (2012) .

[2] W. V. R. Malkus. Precession of the earth as the cause of geomagnetism: Experiments lend support to the proposal that precessional torques drive the earth's dynamo. Science, 160(3825):259–264, 1968.

[3] A. Tilgner. Precession driven dynamos. Physics of Fluids, 17(3):034104, 2005.

[4] C.-C. Wu and P. Roberts. On a dynamo driven by topographic precession. Geophysical & Astrophysical Fluid Dynamics, 103(6):467–501, 2009.

[5] J.-L. Guermond, R. Laguerre, J. Léorat, and C. Nore. Nonlinear magnetohydrodynamics in axisymmetric heterogeneous domains using a Fourier/finite element technique and an interior penalty method. J. Comput. Phys., 228:2739–2757, 2009.

[6] J. L. Guermond, J. Léorat, F. Luddens, C. Nore and A. Ribeiro, Effects of discontinuous magnetic permeability on magnetodynamic problems, J. Comp. Physics 230 (2011) 6299–6319.

[7] C. Nore, J. Léorat, J. L. Guermond and F. Luddens : Nonlinear dynamo action in a precessing cylindrical container, Physical Review E 84, 016317, 2011.